



**HAL**  
open science

## Orientation and Alignment Echoes

G. Karras, E. Hertz, F. Billard, B. Lavorel, J.-M. Hartmann, O. Faucher, Erez  
Gershnel, Yehiam Prior, Ilya Sh. Averbukh

► **To cite this version:**

G. Karras, E. Hertz, F. Billard, B. Lavorel, J.-M. Hartmann, et al.. Orientation and Alignment Echoes. Physical Review Letters, 2015, 114 (15), <10.1103/PhysRevLett.114.153601>. <hal-02398531>

**HAL Id: hal-02398531**

**<https://hal.science/hal-02398531v1>**

Submitted on 7 Dec 2019

**HAL** is a multi-disciplinary open access archive for the deposit and dissemination of scientific research documents, whether they are published or not. The documents may come from teaching and research institutions in France or abroad, or from public or private research centers.

L'archive ouverte pluridisciplinaire **HAL**, est destinée au dépôt et à la diffusion de documents scientifiques de niveau recherche, publiés ou non, émanant des établissements d'enseignement et de recherche français ou étrangers, des laboratoires publics ou privés.



HAL Authorization

# Orientation and Alignment Echoes

G. Karras<sup>1</sup>, E. Hertz<sup>1</sup>, F. Billard<sup>1</sup>, B. Lavorel<sup>1</sup>, J.-M. Hartmann<sup>2</sup>, and O. Faucher<sup>1\*</sup>

<sup>1</sup>Laboratoire Interdisciplinaire CARNOT de Bourgogne,

UMR 6303 CNRS-Université de Bourgogne, BP 47870, 21078 Dijon, France and

<sup>2</sup>Laboratoire Interuniversitaire des Systèmes Atmosphériques (LISA) CNRS (UMR 7583),

Université Paris Est Créteil, Université Paris Diderot, Institut Pierre-Simon Laplace,

Université Paris Est Créteil, 94010 Créteil Cedex, France

Erez Gershnel, Yehiam Prior, and Ilya Sh. Averbukh<sup>†</sup>

Department of Chemical Physics, The Weizmann Institute of Science, Rehovot 76100, Israel

(Dated: March 12, 2015)

We present one of the simplest classical system featuring the echo phenomenon - a collection of randomly oriented free rotors with dispersed rotational velocities. Following excitation by a pair of time-delayed impulsive kicks, the mean orientation/alignment of the ensemble exhibits multiple echoes and fractional echoes. We elucidate the mechanism of the echo formation by kick-induced filamentation of phase space, and provide the first experimental demonstration of classical alignment echoes in a thermal gas of CO<sub>2</sub> molecules excited by a pair of femtosecond laser pulses.

PACS numbers: 45.50.-j, 37.10.Vz, 42.50.Md

Echoes are common in many areas of physics. When an inhomogeneous ensemble of many nonlinear systems is impulsively kicked by an external force, the transient response to the kick vanishes fast due to dispersion in the properties of individual systems. The same happens when the ensemble is kicked again, however a new impulsive response shows up at twice the delay between the two pulses, - a celebrated echo phenomenon first observed by Hahn in precessing nuclear spins [1]. Echoes have been observed in a wide class of classical systems, including cyclotron echo [2, 3], plasma wave echo [4], photon echo [5] and its mechanical analogs [6]. Echoes were predicted to occur in proton storage rings [7, 8], and were observed in high energy hadron beam experiments [9, 10]. Echo-enabled generation of short-wavelength radiation in free-electron lasers [11–13] was demonstrated (for a recent review, see [14]). Echoes are being also discussed in the context of cavity quantum electrodynamics [15, 16] and cold atom systems [17–20].

In this Letter, we identify one of the simplest classical system featuring the echo phenomenon - a collection of free classical rotors stimulated by an external impulsive force. Using geometric arguments on the kick-induced transformations of the rotors phase-space, we predict multiple echoes in the mean orientation/alignment of the ensemble. Our qualitative analysis reveals the echo mechanism and predicts its dependence on parameters of the stimulating kicks. A full analytical theory of these echoes in 2D and 3D thermal ensembles of classical rotors, and its generalization to the quantum case will be published elsewhere [21]. Here, we discuss the physics behind the predicted echo effect and demonstrate it experimentally in a collection of CO<sub>2</sub> molecules stimulated by a pair of femtosecond laser pulses.

For a linear molecule having a permanent dipole mo-

ment  $\mu$ , and driven by a linearly polarized field, the interaction potential leading to orientation is  $V(\theta, t) = -\mu E(t) \cos(\theta)$ , where  $E(t)$  is the field amplitude, and  $\theta$  is the polar angle between the molecular axis and the field direction. In the absence of a permanent dipole moment, the external field couples to the induced molecular polarization. For nonresonant laser fields, the angular-dependent interaction potential is  $V(\theta, t) = -(\Delta\alpha/4)E^2(t) \cos^2(\theta)$  [22, 23], which leads to alignment along the field polarization (for reviews on molecular alignment see [24–28]). Here  $\Delta\alpha$  is polarizability anisotropy, and  $E(t)$  is the *envelope* of the laser pulse. The effects we present here are rather similar for the above two interaction types. Thus, in what follows, we use the dipole interaction form ( $V \sim -\cos(\theta)$ ) for discussion, and point out differences appearing in the case of alignment ( $V \sim -\cos^2(\theta)$ ).

Consider an ensemble of 2D rotors kicked by a short orienting pulse at  $t = 0$ . The angular velocity,  $\omega$  and angle  $\theta$  of a rotor at time  $t$  are given by

$$\omega = \omega_0 - \Omega \sin(\theta_0), \quad \theta = \theta_0 + \omega t \quad (1)$$

Here  $\omega_0, \theta_0$  are the initial conditions, and  $\Omega$  is proportional to the intensity of the kick. The orientation of the ensemble of rotors is quantified by the mean value of  $\langle \cos(\theta) \rangle$ , referred to as the orientation factor. Let us first assume that all the rotors are initially at rest and uniformly distributed in the angular interval  $[-\pi, \pi]$ , as represented by the horizontal blue line in Fig.1. A short kick in the  $\theta = 0$  direction does not move the rotors during its action, but induces rotation with angular speed  $-\Omega \sin(\theta)$  (see Eq.(1)). Immediately after the kick, the phase space distribution of the rotors takes a shape shown by the red curve in Fig.1. In the course of the following free evolution, each point on the red curve moves horizontally towards  $\theta = 0$  with a velocity defined by its

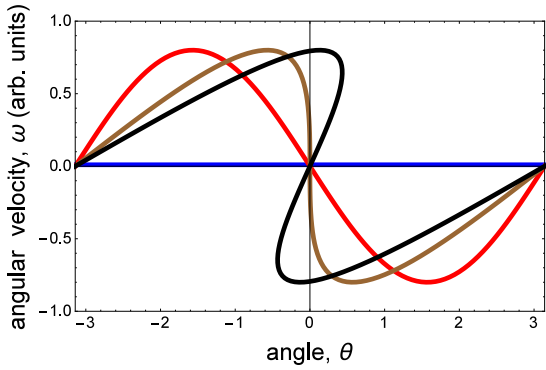


FIG. 1. (color online) Kick-induced orientation of an ensemble of rotors (see text for details).

initial vertical position, as shown by the next two curves. After a certain delay, the curve experiences steepening at  $\theta = 0$  (light green curve), not unlike the accumulation of cars in congested traffic, which leads to a singularity in the angular distribution of the rotors [29]. Note, however, that the maximal value of the orientation factor  $\langle \cos(\theta) \rangle$  is achieved not at this moment, but some time later, when the curve takes a typical folded shape (black curve in Fig.1) leading to increased density of rotors in the region near  $\theta = 0$  [29]. This is a transient orientation, and the stronger the kick the shorter is the time needed to reach the maximally oriented state.

Next, we consider an ensemble that is initially uniformly dispersed in angle, and has a spread in angular velocity  $\omega$ . For certainty, we assume a Gaussian distribution of angular velocities  $f(\theta_0, \omega_0) \sim \exp[-\omega_0^2/(2\sigma^2)]$ . The time-dependent orientation factor after the kick is found to be:  $\langle \cos(\theta)(t) \rangle = \exp[-\sigma^2 t^2/2] J_1(\Omega t)$ , where  $J_1(z)$  is the Bessel function of the first order. This pulsed response disappears fast as  $\sigma t \rightarrow \infty$ . By inverting the map (1) and using its area preserving property, one arrives at the following expression for the probability distribution function at time  $t$ :

$$f(\omega, \theta, t) = \frac{1}{2\pi} \frac{1}{\sqrt{2\pi}\sigma} \exp\left[-\frac{[\omega - \Omega \sin(\omega t - \theta)]^2}{2\sigma^2}\right] \quad (2)$$

Figure 2 shows the transformation of the initial distribution with time. Shortly after the kick (Fig. 2a) the density distribution takes a folded shape similar to the one shown in Fig. 1, resulting in the transient orientation. On the longer time scales, when the orientation signal  $\langle \cos(\theta) \rangle(t)$  vanishes, the probability density becomes rippled and develops multiple parallel filaments (see Fig. 2b). The number of these filaments grows with time, and their width is diminishing in order to keep the occupied phase space volume constant. Eventually, all the filaments tend to become almost horizontal and uniform in density. As follows from Eq.(2), the neighboring filaments are separated in angular velocity by  $2\pi/t$ , where  $t$  is the evolution time.

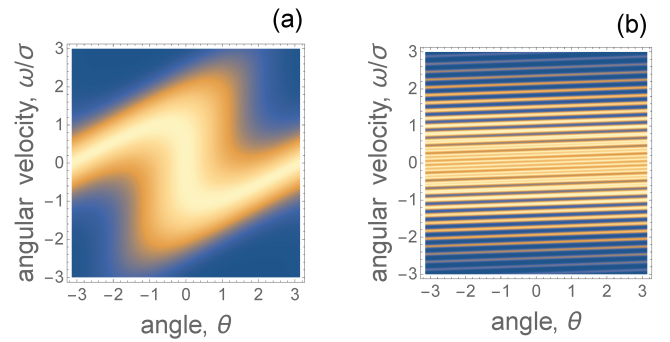


FIG. 2. (color online) Filamentation of the phase space density.  $\Omega/\sigma = 1$ , (a)  $\sigma t = 1$ , (b)  $\sigma t = 30$ .

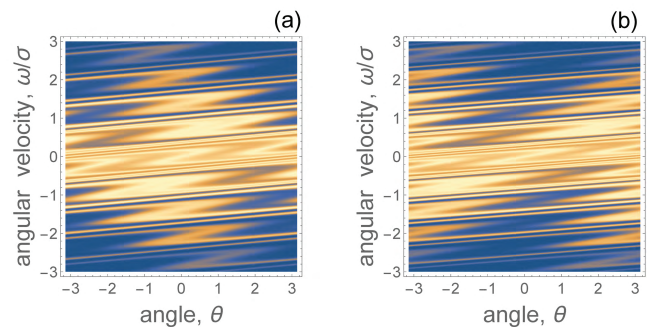


FIG. 3. (color online) Echo formation in the filamented phase space.  $\Omega_1/\sigma = 1$ ,  $\sigma T = 10$ , and  $\Omega_2/\Omega_1 = 1/3$ . Panel (a):  $\sigma\tau = 9.11$  - orientation echo. Panel (b):  $\sigma\tau = 10.85$  - anti-orientation echo.

At  $t = T$ , the ensemble is subject to another kick. Every filament in Fig. 2b is quite analogous to the initial uniform distribution of rotors shown in Fig. 1 by the blue line, but it has a non-zero mean velocity. With time, these filaments form the typical folded patterns leading to the transient orientation of the rotors in the filament. For every angle  $\theta$ , the emerging patterns from neighboring filaments start moving with the velocity difference  $2\pi/T$  with respect to each other. As a result, the kick-induced patterns are generally shifted with respect to each other most of the time after the kick, which results in a quasi-uniform total angular distribution considered as a function of  $\theta$  only. However, at time  $\tau \sim T$  after the second kick, the folded filaments synchronously pile up near  $\theta = 0$  due to the above “quantization” of the angular velocities of the strips (see Fig. 3a). This results in an echo in the orientation factor  $\langle \cos(\theta) \rangle$ . Figure 3b demonstrates also orientation along  $\theta = \pi$  that happens a little bit later in the same time region (anti-orientation echo).

These qualitative arguments have a considerable predictive power, in particular, the same mechanism should

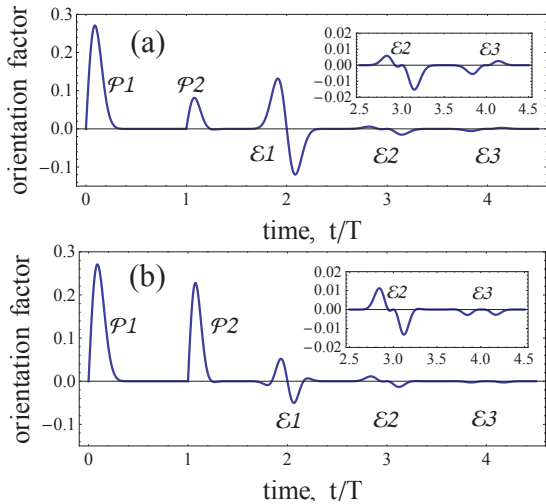


FIG. 4. (color online) Orientation factor versus time after the first kick.  $\Omega_1/\sigma = 1$ ,  $\sigma T = 10$ . Panel (a):  $\Omega_2/\Omega_1 = 1/3$ . Panel (b):  $\Omega_2/\Omega_1 = 1$ . Here  $\mathcal{P}1$  and  $\mathcal{P}2$  denote transient responses to the first and the second kick, respectively.  $\mathcal{E}1$ ,  $\mathcal{E}2$  and  $\mathcal{E}3$  are echoes of the first, second, and third order, respectively. Insets show a magnified view of the second and third echoes.

form the echo signals also at delays  $2T, 3T, \dots$  after the second pulse (higher order echoes). Moreover, it is expected that synchronization of the patterns from non-neighboring strips at  $\tau = T/2, T/3, \dots$  causes highly symmetric structures in the phase space, which may be associated with “fractional echoes”. These echoes are not seen in a mere orientation signal  $\langle \cos(\theta) \rangle$ , but require measuring higher order observables  $\langle \cos(n\theta) \rangle$  ( $n > 1$ ). Moreover, just looking at the phase space pattern at the moment of the main echo, Fig. 3a, one may expect that the echo is best manifested if the delay  $T$  coincides with the time needed for achieving the maximal orientation in every strip. This means that for a given delay there exists a second-kick intensity that maximizes the echo signal.

The simple 2D model considered here (see Eq.(1)) allows for obtaining an analytical expression for the time-dependent mean value of  $\langle \cos(n\theta) \rangle$  where  $n$  is an integer:

$$\langle \cos(n\theta) \rangle(\tau) = \sum_{k=0}^{k=\infty} (-1)^k e^{-\frac{1}{2}\sigma^2(n\tau - kT)^2} J_{k+n}[\Omega_2 n \tau] J_k[\Omega_1(n\tau - kT)] \quad (3)$$

For  $n = 1, 2$  this quantity is the orientation factor and the alignment factor, respectively. Equation (3) presents a sequence of signals localized in time near  $\tau = \frac{k}{n}T$  where  $k$  is an integer. For  $n > 1$ , these are the above mentioned “fractional echoes”, while  $n = 1$  corresponds to the regular orientation echoes. Figure 4 presents calculated time-dependent orientation factor for two values of

the intensity of the second kick. In Figure 4a, the intensity of the second kick,  $\Omega_2$  was optimized to achieve the maximal amplitude of the main echo at  $\tau \sim T$ . Although the second kick in Fig. 4a is three times weaker than that of Fig. 4b, it induces a considerably stronger echo, that even exceeds the initial response to the second kick. The peak and dip of the first echo in Fig. 4a correspond to the left and right panel of Fig. 3, respectively. As follows from Eq. (3), the amplitude of the echo is a decaying oscillatory function of the intensity of the second kick,  $\Omega_2$  after reaching the global maximum shown at Fig. 4a.

The same qualitative mechanism works in the case of the polarization-induced interaction ( $V \sim -\cos^2(\theta)$ ), and it produces echoes in the alignment signal,  $\langle \cos^2(\theta) \rangle(t)$ . An analytical expression for the alignment echoes for 2D rotors is provided in the Supplementary Material [31], and it is quite similar to the Eq.(3). The visualization of the phase space transformations in the case of alignment is more involved, but the main results remain the same, including the non-monotonous dependence of the echo signals on the intensity of the second kick.

We note the remarkable similarities between the physics of laser-induced alignment/orientation of molecules [24–28] and modern techniques for laser manipulations over electron beams in accelerator-based light sources [11–14]. Both research fields aim at compressing the density of particles in certain areas (angular alignment/orientation vs electron bunching along the beam) by laser pulses, and in both cases phase-space folding is involved [11, 14, 29, 30]. The orientation/alignment echoes described here have much in common with the phenomena involved in echo-enabled harmonics generation (EEHG) in free-electron lasers. This connection is not merely formal, and may be beneficial for both fields. In particular, recent proposals to use several laser fields to significantly increase the electrons bunching factor [14] may be supported by a similar suggestion [29, 30] in the context of molecular orientation/alignment by series of laser pulses. This concept was theoretically optimized [32], experimentally demonstrated [33–35], and even successfully applied to the enhanced focusing (bunching) of cold atoms interacting with multiple laser fields [36, 37].

In what follows, we describe the first experimental observation of the rotational alignment echoes in laser-kicked  $\text{CO}_2$  molecules. The details of our experimental setup [38] are described in the Supplementary Material [31]. The two linearly polarized pump pulses  $\mathcal{P}1$  and  $\mathcal{P}2$  are derived from an amplified Ti:Sapphire laser (1 kHz, 800 nm, 100 fs FWHM) and properly delayed before being focused inside a  $\text{CO}_2$  filled gas cell at a pressure of 0.2 bar. The alignment echoes are observed by time-resolved birefringence measurements [39], where a delayed, weak probe pulse, linearly polarized at  $+45^\circ$  relative to the pump pulses is linearly analyzed after passing

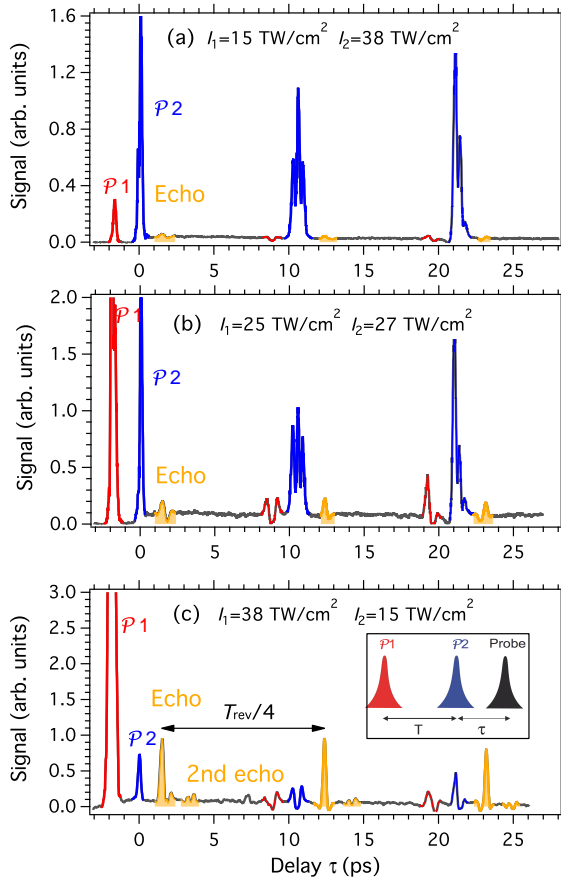


FIG. 5. (color online) Birefringence signals as a function of the pump-probe delay  $\tau$  for different intensities  $I_1$  and  $I_2$  of the pump pulses  $\mathcal{P}1$  and  $\mathcal{P}2$ , respectively (see the inset).  $T_{\text{rev}}$ : rotational revival time.

through the cell by a polarizer set at  $-45^\circ$  relative to the pump pulses. The birefringence signal measured on the detector can be written as [40]

$$\mathcal{S}(\tau) \propto \int_{-\infty}^{\infty} I_{\text{pr}}(t - \tau) \left[ \langle \cos^2(\theta) \rangle(t, I_1, I_2) - \frac{1}{3} \right]^2 dt \quad (4)$$

where  $\langle \cos^2(\theta) \rangle(t, I_1, I_2)$  is the alignment factor, and  $I_1$ ,  $I_2$ , and  $I_{\text{pr}}$ , are the intensity of  $\mathcal{P}1$ ,  $\mathcal{P}2$ , and the probe pulse, respectively.

Figure 5 presents the pump-probe signals obtained for three different sets of pump intensities with a delay  $T$  between  $\mathcal{P}1$  and  $\mathcal{P}2$  set to 1.6 ps. We measured the alignment signals till about one-half of the rotational revival time,  $T_{\text{rev}}$  of the  $\text{CO}_2$  molecule ( $T_{\text{rev}} \sim 42.7$  ps). The classical echo effects discussed in this paper happen within the time interval of about  $T_{\text{rev}}/4$  where the alignment dynamics is well described by the classical mechanics. To guide the eye, the alignment signals caused by the pulses  $\mathcal{P}1$  and  $\mathcal{P}2$ , and also their one-quarter and one-half revivals are colored in red and blue, respectively, whereas

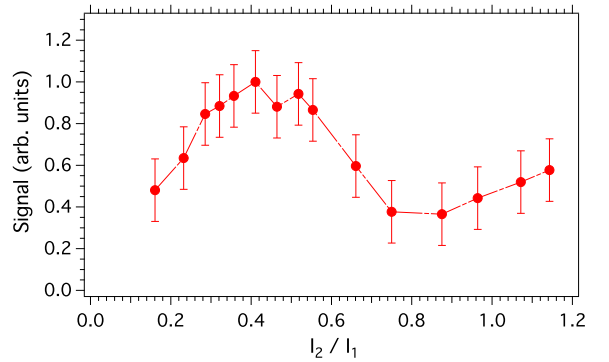


FIG. 6. (color online) Peak amplitude of the birefringence signal for the echo near  $\tau = T$  versus  $I_2/I_1$ , with  $I_1$  set to  $44 \text{ TW/cm}^2$ .

the echoes are highlighted with a yellow color. For each intensity set, an echo is produced after  $\mathcal{P}2$  at  $\tau \sim T$ . Its amplitude depends on the intensities of both  $\mathcal{P}1$  and  $\mathcal{P}2$ . The maximum echo amplitude seen in Fig. 5c is achieved for a second pulse that is weaker than the first one,  $I_2/I_1 \sim 0.4$ , and this echo is stronger than the initial response induced by the second pulse  $\mathcal{P}2$ . These observations resemble the theoretical results shown in Fig. 4, and they may be understood using the similar qualitative arguments. The second echo produced at  $\tau \sim 2T$  is also visible in Fig. 5c. On the longer time scale, replicas of these echoes are observed near the quarter and half-revival regions. They appear due to the interplay between the classical echo effect and the phenomenon of fractional quantum revivals [41]. These replicas will not be discussed in detail here, but they are nicely reproduced in the fully quantum theoretical description of our experiments (to be published). Related transient signals were also reported in Ref. [42] where the alignment of  $\text{N}_2\text{O}$  molecules excited by two strong femtosecond laser pulses was studied. In these experiments the delay between the pulses was chosen close to the quarter-revival time, far beyond the region where the classical echo effects of the present paper exist. In order to reveal the non-monotonic dependence of the echo amplitude, we varied the intensity of the second pulse  $\mathcal{P}2$  while keeping the first one ( $\mathcal{P}1$ ) fixed. The results are summarized in Fig. 6 that demonstrates the existence of an optimal intensity of the second kick, and the oscillatory dependence of the echo amplitude on this intensity, in agreement with our theoretical considerations.

Summarizing, we showed that a textbook classical system - a collection of randomly oriented free rotors with dispersed rotational velocities - exhibits multiple echoes of different kinds in its orientation/alignment dynamics when kicked by a pair of delayed pulses. We provided qualitative and quantitative analysis of the phenomenon using a simple model system, and performed the first

experimental demonstration of the classical alignment echoes in a thermal gas of CO<sub>2</sub> molecules excited by a pair of femtosecond laser pulses. The echoes were observed on a time scale much shorter than the quantum revival time, and their parameters were readily controllable by the intensity and delay of the excitation pulses. This makes the orientation/alignment echoes promising for exploring relaxation processes in high pressure gases and various liquids, including superfluid helium [43], where quantum rotational responses are considerably suppressed.

This work was supported by the Conseil Régional de Bourgogne (PARI program), the CNRS, the Labex ACTION program (contract ANR-11-LABX-01-01), and the French National Research Agency (ANR) through the CoConicS program (Contract No. ANR-13-BS08-0013). This research was also supported by DFG (Project No. LE 2138/2-1) and Minerva Foundation. I.A. acknowledges kind hospitality and support from the Université Paris Est Créteil during a one week stay at LISA.

---

\* olivier.faucher@u-bourgogne.fr

† ilya.averbukh@weizmann.ac.il

- [1] E.L. Hahn, Phys. Rev. **80**, 589 (1950).
- [2] R.M. Hill, and D.E. Kaplan, Phys. Rev. Lett. **14**, 1062 (1965).
- [3] R.W. Gould, Phys. Lett. **19**, 477 (1965).
- [4] R.W. Gould, T.M. O'Neil, J.H. Malmberg, Phys. Rev. Lett. **19**, 219 (1967).
- [5] N.A. Kurnit, I.D. Abella, and S.K. Hartmann, Phys. Rev. Lett. **13**, 567 (1964).
- [6] V. P. Chebotayev and B. Ya. Dubetsky, Appl. Phys. B **31**, 45 (1983).
- [7] G.V. Stupakov, "Echo Effect In Hadron Colliders", SSC Report SSCL-579, July 1992.
- [8] G.V. Stupakov and S. Kauffmann, "Echo Effect in Accelerators", SSC Report SSCL-587, September 1992.
- [9] L. K. Spentzouris, J. F. Ostiguy, and P. L. Colestock, Phys.Rev. Lett. **76**, 620 (1996).
- [10] O. Bruning, T. Linnecon, F. Ruggio, W. Scandale, and E. Shaposhnikova, *Nonlinear and Collective Phenomena in Beam Physics* (AIP, New York, 1997), p. 155.
- [11] G. Stupakov, Phys. Rev. Lett. **102**, 074801 (2009).
- [12] D. Xiang et al., Phys.Rev.Lett. **105**, 114801 (2010).
- [13] Z.T. Zhao et al., Nature Photonics **6**, 360 (2012).
- [14] E. Hemsing, G. Stupakov, and D. Xiang, Rev. Mod. Phys. **86**, 897 (2014).
- [15] G. Morigi, E. Solano, B.-G. Englert, and H. Walther, Phys. Rev. A **65**, 040102 (2002).
- [16] T. Meunier, S. Gleyzes, P. Maioli, A. Auffeves, G. Nogues, M. Brune, J. M. Raimond, and S. Haroche, Phys. Rev. Lett. **94**, 010401 (2005).
- [17] A. Bulatov, A. Kuklov, B.E. Vugmeister, and H. Rabitz, Phys. Rev. A **57**, 3788 (1998).
- [18] F.B.J. Buchkremer, R. Dumke, H. Levsen, G. Birkl, and W. Ertmer, Phys. Rev. Lett. **85**, 3121 (2000).
- [19] M.F. Andersen, A. Kaplan, and N. Davidson, Phys. Rev. Lett. **90**, 023001 (2003).
- [20] M. Herrera, T.M. Antonsen, E. Ott, and S. Fishman, Phys. Rev. A **86**, 023613 (2012).
- [21] G. Karras, E. Hertz, F. Billard, B. Lavorel, J.-M. Hartmann, O. Faucher, E. Gershnel, Y. Prior, and I. Sh. Averbukh, (to be published)
- [22] R.W. Boyd, *Nonlinear Optics* (Academic Press, Boston, 1992).
- [23] B. Friedrich and D. Herschbach, Phys. Rev. Lett. **74**, 4623 (1995); J. Phys. Chem. **99**, 15 686 (1995).
- [24] H. Stapelfeldt and T. Seideman, Rev. Mod. Phys. **75**, 543 (2003)
- [25] Y. Ohshima and H. Hasegawa, Int. Rev.Phys. Chem. **29**, 619 (2010).
- [26] S. Fleischer, Y. Khodorkovsky, E. Gershnel, Y. Prior, and I. Sh. Averbukh, Isr. J. Chem. **52**, 414 (2012).
- [27] M. Lemeshko, R. V. Krems, J. M. Doyle, S. Kais, Mol. Phys. **111**, 1648 (2013).
- [28] S. Pabst, The European Physical Journal Special Topics, **221**, 1-71 (2013).
- [29] I. Sh. Averbukh and R. Arvieu, Phys. Rev. Lett. **87**, 163601 (2001).
- [30] M. Leibscher, I. Sh. Averbukh, P. Rozmej, and R. Arvieu, Phys. Rev. A **69**, 032102 (2004).
- [31] see the Supplemental Material at [URL will be inserted by publisher] for the analytical expression for the alignment echoes in 2D model with the polarization-induced interaction, and for the details of the experimental setup.
- [32] M. Leibscher, I. S. Averbukh, and H. Rabitz, Phys. Rev. Lett. **90**, 213001 (2003); Phys. Rev. A **69**, 013402 (2004).
- [33] C.Z. Bisgaard, M.D. Poulsen, E. Péronne, S.S. Viftrup, and H. Stapelfeldt, Phys.Rev.Lett **92**, 173004 (2004).
- [34] K.F. Lee, I.V. Litvinyuk, P.W. Dooley, M. Spanner, D.M. Villeneuve, and P.B. Corkum, J. Phys. B: At. Mol.Opt. Phys. **37**, L43 (2004).
- [35] M. Renard, E. Hertz, S. Guérin, H. R. Jauslin, B. Lavorel, and O. Faucher, Phys.Rev. A **72** 025401 (2005).
- [36] M. Leibscher and I. Sh. Averbukh, Phys. Rev. A **65**, 053816 (2002).
- [37] W.H. Oskay, D.A. Steck, and M.G. Raizen, Phys.Rev.Lett. **89**, 283001 (2002).
- [38] G. Karras, E. Hertz, F. Billard, B. Lavorel, J.-M. Hartmann, and O. Faucher, Phys. Rev. A **89** 063411 (2014).
- [39] V. Renard, M. Renard, S. Guérin, Y. T. Pashayan, B. Lavorel, O. Faucher, and H. R. Jauslin, Phys. Rev. Lett. **90**, 153601 (2003).
- [40] O. Faucher, B. Lavorel, E. Hertz, and F. Chaussard, in it Progress in Ultrafast Intense Laser Science, vol. VII (Springer, 2011), vol. 100 of *Springer Series in Chemical Physics*, pp. 79-108.
- [41] I.Sh. Averbukh and N.F. Perelman, Phys. Lett. A **139**, 449 (1989).
- [42] H. Jiang, C. Wu, H. Zhang, H. Jiang, H. Yang and Q. Gong, Opt. Express **18**, 8990 (2010).
- [43] D. Pentlechner, J. H. Nielsen, A. Slenczka, K. Mølmer, and H. Stapelfeldt, Phys. Rev. Lett. **110**, 093002 (2013).